PROCEEDINGS, Twenty-Seventh Workshop on Geothermal Reservoir Engineering
Stanford University, Stanford, California, January 28-30, 2002
SGP-TR-171

NEW INTERPRETATIONS OF GEOTHERMAL FLUID INCLUSION VOLATILES: AR/HE AND N_2/AR RATIOS - A BETTER INDICATOR OF MAGMATIC VOLATILES, AND EQUILIBRIUM GAS GEOTHERMOMETRY

Nigel Blamey and David Norman

New Mexico Tech
Dept. E&ES
Socorro, NM 87801
e-mail: nblamey@nmt.edu

ABSTRACT

N_2/Ar and Ar/He relationships:

Fluid inclusion magmatic gases are measured using quadrupole mass spectrometers and the data is compared to measurements of volcanic gas analyses. Data reported by Giggenbach from active volcanoes give N_2/Ar ratios in the general range of 100 to 1000 whereas corresponding Ar/He ratios vary from 100 to 2. Plotted on a Ar/He vs. N_2/Ar diagram the data defines a field that has a negative slope. Fluid inclusion gases from Mt. Erebus anorthoclase and analyses of magmatic gas-filled inclusions provided by Jake Lowenstern also plot within the same field. Thus we considered the Ar/He-N_2/Ar field outline by volcanic gases and magmatic inclusion analyses to represent magmatic gases. The trend in the data is attributed to the stronger partitioning of Ar into the gas phase and as a magmatic system evolves; thus Ar becomes more rapidly depleted from the melt than N_2 and He. The advantage of Ar/He vs. N_2/Ar plots is that they discriminate between fluids that have magmatic N_2/Ar ratios from admixed organic N_2.

Hansonburg MVT (Mississippi Valley Type) deposit fluid inclusions have Ar/He ratios of 0.12 to 2.69 and N_2/Ar ratios ranging from 69 to 182, and the ratios >100 might suggest a magmatic component. However, MVT deposits generally have some inclusions filled with hydrocarbon compounds, as does the Hansonberg deposit (ref), and MVT ore fluids are considered to be amagmatic and sedimentary in origin (ref). When plotted on a Ar/He-N_2/Ar plot Hansonberg gas analyses plot outside the magmatic box. The same is true for Coso analyses that have some N_2/Ar greater than 1000. One third of the gas data analyses from Broadlands plot within the magmatic box. The Geysers analyses plot both in and below the magmatic box and can be explained in terms of mixing between magmatic and a crustal component.

Geothermometry:

With the improved capability to make accurate fluid inclusion H_2 analyses we have applied the following equilibrium gas geothermometers to our fluid inclusion gas analyses.

$$C + 2H_2O = 2H_2 + CO_2 \quad .....(1)$$

$$2H_2O + CH_4 = CO_2 + 4H_2 \quad .....(2)$$

The assumptions for fluid inclusion gas geothermometry are equilibrium conditions at the time of trapping, a single fluid, no boiling occurred, and that species have not reacted nor were lost after trapping. Gas geothermometry based on equation 1 applied to Hansonburg fluorite gives temperatures of 157 to 308 ºC average 245±47 ºC 1σ whereas the fluid inclusion Th's range from 147 to 229 ºC and average 182±20 ºC 1σ. Hansonburg inclusions show no evidence of boiling, however, necking is common and gas data suggest two fluids. The Th distribution is attributed in part to inclusion necking. Snowbird pegmatite quartz inclusions show no evidence of boiling. Equilibrium gas geothermometry values ranging from 384 to 463 ºC (2) and average 437±25 ºC 1σ. Similarly, values range from 350 to 421 ºC (1) and average 395±23 ºC 1σ, whereas Tt is estimated at 420 ºC from microthermometry. A Karaha quartz analysis from drill hole T-8, 794.7m give temperatures of 270 (1) and 293 (2). There is no thermometric data on this sample, however Th values for other quartz samples range from 280 to 330 ºC. In conclusion fluid inclusion gas geothermometry can be applied with caution provided that H_2 analyses are accurate, fluid inclusion necking is absent, and there is no indication of fluid boiling or trapping multiple fluids.

This paper is subdivided into two parts, one that addresses the use of N_2-Ar-He gas ratios in identifying a field common to magmatic sources. The second aspect deals with the application of gas

geothermometry to fluid inclusion gas analysis. Both subjects being addressed require data collected by analyzing the gases trapped within fluid inclusions.

INTRODUCTION

This paper is the seventh presented at the Stanford Geothermal Workshop whose subject is the interpretation of geothermal fluid sources and processes from gaseous species. Here we discuss a new method of identifying magmatic-derived fluids, an improvement on measuring magmatic gases in magmatic-glass inclusions, and look at the possibility of applying equilibrium gas geothermometry to fluid inclusion analyses.

The N_2/Ar ratio is used to identify magmatic contributions to geothermal fluids. The problem with use of this ratio is that N_2 can also be derived from organic compounds. Plots of N_2/Ar vs. CO_2/CH_4 are used to differentiate between magmatic fluids and crustal-derived fluids that have "magmatic" N_2/Ar ratios. The weakness in this approach is that it assumes that most methane is sedimentary in origin, whereas there is abundant evidence that methane may be produced by inorganic processes. Thus there is a need for a better method of identifying magmatic gas in geothermal systems that uses less reactive gaseous species. Here we will present data that shows that Ar-He-N_2 ratios fingerprint magmatic volatiles better than the N_2-Ar ratio alone.

The strong association of active magmatic systems and geothermal systems warrants investigation into the chemical signatures that characterize these fluids. To improve our understanding of geothermal systems there is the need to identify fluid inputs, particularly magmatic fluids since hot igneous bodies provide the heat that drive geothermal systems. Collecting gas samples from volcanoes for analysis can be hazardous whereas analyzing fluid inclusions offers a much safer alternative to sample collection.

Magmatic Volatiles

The analysis of gases venting from volcanoes has been of interest for many years primarily resulting from the threat to human life in close proximity to active volcanoes. Initial data collection focused on CO_2, SO_2, H_2S and water, however, with time the suite of gases has expanded to include He, CH_4, N_2, Ar and others. Several researchers have been involved in collection of gas data venting from active volcanoes, the major areas of interest being related to convergent plate boundaries. But there is relatively few good analyses of the entire suite of volcanic gases, in part because of the problems with air contamination. Analysis of magmatic glass inclusions holds promise to provide magmatic gas analyses, but analytical problems remain. Most analyses of magmatic volatiles have therefore focused on limited volatiles such as water, chlorine, and helium (compilation by Giggenbach, 1996). Norman and Moore (1997) reported that crushing magmatic glass inclusions gave unsatisfactory results because of air contamination presumably trapped in cooling fractures in the quartz phenocrysts they used.

Magmatic Gas Ratios

The CO_2/CH_4 vs. N_2/Ar diagram developed by Norman et al. (1999) is used to differentiate fluid inclusion gases into fields that include a magmatic, meteoric, crustal, and crustal-organic zones (fig. 1). Air saturated water (ASW) at 20 ºC has a N_2/Ar ratio of 38, meteoric waters have ratios as high as 54 from the vadose zone. Additions of air, and fractionation from fluid boiling can change meteoric fluid ratios resulting in ratios from about 25 to about 105 (Norman et al., 1997), whereas Giggenbach shows that subduction-related volcanoes have N_2/Ar ratios from about 100 to >1000. Atmospheric ratios of CO_2/CH_4 are around 8000 but as meteoric water enters the crust, the fluid comes into equilibrium with the anaerobic conditions causing the methane content to increase. Magmatic fluid compositions have water as the major component followed by CO_2 and similarly, as a magmatic fluid interacts with the crust, the CO_2/CH_4 ratio decreases. The organic field on the diagram recognizes that biotic material contains nitrogen, hence that methane added to geothermal fluids by pyrolysis of sedimentary organic compounds will add nitrogen as well, thus increase the N_2/Ar ratio. Experiments show that reaction of hot waters with rocks may produce methane by Fischer-Tropsch reactions (Berndt et al., 1996). In Carlin-style gold mineralization Blamey (2000) identified CO_2 loss by wall-rock interaction as the most critical process in decalcification. Thus, both CO_2 and CH_4 are components that can be lost or gained in the crust and are therefore a weaknesses to the use of the CO_2/CH_4-N_2/Ar diagram. Gaseous species that are less reactive than CO_2 and CH_4, and do not combine with rock-forming minerals are better for categorizing magmatic and meteoric fluids. Hence, we here look at ratios of Ar/He plotted against the N_2/Ar. A compilation of gas data from volcanoes located on convergent plate boundaries is presented by Giggenbach (1996) and their Ar/He and corresponding N_2/Ar ratios are shown in figure 2. A frame defining the outline of Giggenbach's compiled data is used in further figures.

Gas Geothermometry

The idea of using geothermal fluid gas ratios is not new. The principle is that of assuming equilibrium concentrations of gaseous species produced in the liquid or gas phase at various temperatures by geothermal fluids. An assumption applies in that the equilibrium reaction goes in one direction and that gas concentrations reflect the highest equilibrium

temperature. Most commonly gas equilibrium geothermometers are applied to gaseous species dissolved in the liquid phase. We follow this convention when applying gas geothermometry to fluid inclusion gas analyses because it is unclear if equilibrium conditions are maintained in boiling geothermal fluids. Strictly speaking, the use of gas concentration should be replaced with gas fugacity since equilibrium gas concentrations are changed by fluid salinity. The assumptions for fluid inclusion gas geothermometry are equilibrium conditions at the time of trapping, homogeneous trapping of a single fluid, no boiling occurred, and that species have not reacted nor were lost after trapping, and fluid salinity is known. The later condition is necessary because equilibrium gas concentrations change with fluid salinity. In the following discussions it is assumed that salinity is near zero, as is the case with many geothermal fluids. Although there are a number of gas geothermometers that can be applied, we will address the following two reactions since our mass spectrometers routinely measure the principle gaseous species:

$C + 2H_2O = 2H_2 + CO_2$ .....(1)

$2H_2O + CH_4 = CO_2 + 4H_2$ .....(2)

Unlike the geothermal systems where gases are collected in large vessels, we are applying the gas geothermometer principles to micron-sized fluid inclusions that are trapped within minerals. The scale of the sample is many orders of magnitude smaller. Our objective will be to test whether gas geothermometry can be meaningfully applied to fluid inclusions, and if the results are meaningful.

Gas geothermometers and their application to geothermal systems are described by Giggenbach (1980) and D'Amore and Panichi (1980). In many cases these systems have low salinity and the "salting-out" effects are not mentioned. Nehring and D'Amore (1984) report that the Fischer- Tropsch reaction (2) predicts temperatures greater than reservoir fluids, and application of this reaction to The Geyser steam predicts temperatures higher than reservoir steam. However, Henley et al. (1984) demonstrate quite accurate results with this geothermometer. Reaction (1) is less sensitive to hydrogen measurement and salinity than reaction (2). Application to the same Cerro Preito analyses studied by Nehring and D'Amore (1984) indicated temperatures near that of reservoir fluids.

METHODOLOGY

Samples were provided a number of sources. Jake Lowenstern provided quartz that host magmatic gas inclusions so large they visible under binocular microscope. Anorthoclase crystals collected at the Mt. Erebus volcano were provided by Jean Wardell. Other samples were collected from the Snowbird pegmatite in Montana and the Victoria porphyry and skarn system in New Mexico. A variety of minerals including quartz, anhydrite, calcite, wairakite, epidote, tremolite and pyrite from geothermal systems were provided by Joe Moore and Sue Lutz.

The analysis of volatile species is done in vacuum by using the CFS (crush-fast scan) method (Norman and Sawkins, 1987). Samples are cleaned with potassium hydroxide, distilled water, and then oven dried at about 60°C (at 100°C He is rapidly lost). Erebus inclusions were removed from the interior of several cm phenocrysts in order to minimize air-filled cracks. Lowenstern material was delivered hand-picked.

Cleaned samples are placed in crushers and evacuated while heating to about 60°C until a pressure $<10^{-7}$ Torr (10^{-8} mPascals) is attained. The analysis is performed by means of a Balzers QME125 quadrupole and Pfeiffer Vacuum Prisma mass spectrometers operating in a fast-scan, peak-hopping mode. The CFS method involves opening inclusions by a swift crush in the vacuum chamber housing the mass spectrometers. Volatiles released are quickly removed by the vacuum pumping system within two sec. Meanwhile, the pulse of inclusion volatiles is recorded by operating the quadrupoles in a fast scan mode with measurements every 200 to 250 msec. The mass peak areas are used to determine the concentration of each specie using predetermined sensitivity factors, peak-stripping algorithms and matrix-inversion programs designed in-house. Opening a 10-20 μm inclusion or group of smaller inclusions of equivalent volume, provides the ideal amount of volatiles for CFS analysis. Five to fifteen sequential crushes are made on a ~200 mg sample. Species routinely recorded are H_2, He, CH_4, H_2O, N_2, O_2, H_2S, Ar, CO_2, SO_2 and C_1-C_4 alkanes and alkenes, cyclopentane, toluene and benzene. The instrument is calibrated with commercial gas mixtures, artificial inclusions filled with gas mixtures, and an in-house fluid inclusion standard. The gas water ratio of the standard inclusions (HF1) is known to about 0.1% by Penfield-tube analysis, thus allowing water calibration with an error less than 0.2%. Measurement precision is <5% for major gaseous species and ~10% for the minor species.

RESULTS

Ar/He-N_2/Ar Ratios:

Little or no oxygen was detected when magmatic inclusions were measured. Analyses of Erebus and Lowenstern's samples plot in the same field on a Ar/He-N_2/Ar diagram (fig. 3) as analyses of andesitic volcanic gases compiled by Giggenbach (1996) (fig. 2).

The negative slope on the plot of magmatic Ar-He-N_2 ratios may be explained by gas partitioning from a magma. Argon partitions more strongly into a vapor phase during boiling than does He and N_2, which have approximately equal partitioning coefficients (Prini and Crovetto (1989). It seems likely that as vesiculation commences in a magma, Ar will become preferentially enriched in the early vapor thereby relatively depleting Ar in the magma. As the magmatic system continues to cool and the fluids evolve, Ar becomes scrubbed from the system decreasing relative to N_2 and He. Thus low N_2/Ar and high Ar/He ratios should indicated early released volatiles, and vice versa for high N_2/Ar ratios.

We plot fluid inclusion analyses of geothermal systems past and active on diagrams similar to figure 3 in order to test the concept of using a Ar/He-N_2/Ar to interpret fluid inclusion analyses. Coso analyses from borehole 83-16, depth 5300 to 10000 ft have N_2/Ar >100 plot in the frame defined by the Giggenbach data (fig. 4), whereas analyses above 4100 ft have N_2/Ar <100 and higher Ar/He than Giggenbach's values. Karaha analyses from K-33 have N_2/Ar about 100 (fig. 5). Some have magmatic Ar/He and some do not. Data from Darajat plot both in the center and up from the field defined by Giggenbach's volcanic data (fig. 6). Hansonburg MVT deposit have Ar/He ratios of 0.12 to 2.69 and N_2/Ar ratios ranging from 69 to 182 (fig. 7) and plot well outside of the volcanic box.

Gas Geothermometry:

Gas geothermometry based on equation 1 applied to Hansonburg fluorite gives temperatures of 157 to 308 ºC average 245±47 ºC 1σ whereas the fluid inclusion Th's range from 147 to 229 ºC and average 182±20 ºC 1σ. Hansonburg inclusions show no evidence of boiling, however, necking is common and gas data suggest two fluids. The Th distribution is attributed in part to inclusion necking. Snowbird pegmatite quartz inclusions show no evidence of boiling. Equilibrium gas geothermometry values ranging from 384 to 463 ºC (2) and average 437±25 ºC 1σ. Similarly, values range from 350 to 421 ºC (1) and average 395±23 ºC 1σ, whereas Tt is estimated at 420 ºC from microthermometry. Karaha quartz analyses from drill hole T-8, 794.7m give geothermometer temperatures of 270 ºC(1) and 293 ºC(2). There is no thermometric data on this sample, however Th values for other quartz samples range from 280 to 330 ºC.

Samples from the Victoria porphyry system near Gage NM, give Th measurements of 177±29 ºC whereas gas geothermometry give 259±33 ºC(1) and 256±44 ºC(2). Microthermometry based on a sample from the associated skarn gives 289±23 ºC whereas gas geothermometry gives 412 ±23 ºC and 452 ±32 ºC.

DISCUSSION

Ar/He-N_2/Ar

The volcanic gas data compiled by Giggenbach (1996) is clearly magmatic in origin and defines a field that we propose is a magmatic field for Ar/He vs. N_2/Ar. Gas data from geothermal systems that are clearly associated with magmas also plot within this magmatic field. Gas data from basalts do not conform to the proposed magmatic field. The N_2/Ar ratio is generally below 100 and the Ar and He content is approximately equal. It would appear that the tectonic setting, sources and processes that control the gases differ between calc-alkaline and tholeiitic volcanism.

There is a advantage to using Ar/He-N_2/Ar plots for magmatic fluid recognition compared to the N_2/Ar ratio alone. Hansonburg data shows that geothermal fluids that have interacted with organic material and have "magmatic" N_2/Ar > 100 do not plot in the volcanic field compiled by Giggenbach (1996). Hence, these data suggest that the Ar/He - N_2/Ar better differentiates magmatic fluids than solely relying on N_2/Ar ratios.

The Karaha geothermal system is located on the margins of an active volcano. The N_2/Ar ratios in the inclusion of about 100 could be interpreted as either meteoric or magmatic. However, analyses plotted on the Ar/He-N_2/Ar diagram (fig. 5) indicate a substantial magmatic component which agrees with the geological environments.

Coso fluid inclusion analyses with N_2/Ar ratios have substantial methane. When plotted on a CO_2/CH_4-N_2/Ar diagram (Norman et al. 2001) data suggest meteoric and either an crustal or evolved magmatic source. The Ar/He-N_2/Ar shows that the second fluid source is magmatic (fig. 4). We have done many other plots of fluid inclusion data that can not be shown here and fluids that have magmatic N_2/Ar generally plot in the magmatic box on Ar/He-N_2/Ar diagrams. Inclusion gases that are suspected to be non-magmatic like those of Hansonburg do not plot in the magmatic box. There are two notable exceptions, both past systems and both associated with back-arc or rift related volcanism. Analyses of the Victoria skarn in New Mexico plot on line and to the left of the magmatic box, and analyses of Twin Creeks gold quartz plot on line and two the left of the box.

The Ar/He-N_2/Ar plot may be applied to analyses of magmatic waters. Analyses of several geothermal fluids complied by Giggenbach (1996) plot in the box for most systems.

Figure 4 and 5 plots suggest Coso and Karaha fluid are derived from several sources. We have no other fields labeled on the diagram at present but the analyses here shown suggest that highly evolved fluids that typically have accumulated considerable helium will plot below the magmatic box, whereas meteoric fluids will plot to the left and above the box. Boiling does not greatly fractionate N_2 and Ar, however, calculations show that boiling will fractionate Ar and helium. Helium is a relatively more soluble specie, hence the Ar/He will increase in a boiled fluid whereas the vapor phase will have a higher ratio than the original fluid. Thus much of the variation we see in Coso analyses (fig.4) maybe from boiling rather than multiple fluids.

Many ore deposits are associated with magmatic fluids and for this reason we have selected an MVT deposit to test whether a purely amagmatic fluid might intersect the magmatic field thereby invalidating our proposed magmatic field. All the Hansonburg data plot outside the magmatic field, strengthening our confidence in the proposed field. In contrast, gas data from Karaha, Dixie Valley and Broadlands plot both within and outside the magmatic field indicating both magmatic and other fluid sources.

Geothermometry

Geothermometry based on reaction 1 has only two gaseous species and we must make the assumption that carbon is present. However, reaction 2 does not require the presence of carbon and therefore is possibly the better reaction for geothermometry. Reaction 2 requires a greater accuracy in the measurement of H_2 than CO_2 or CH_4 as there are four hydrogen molecules in the equilibrium reaction and only one CO_2 or CH_4 molecule. Our quadrupole system has about a 5% 1σ error in the CO_2/CH_4 ratio whereas the 1σ error in the H_2 analysis is much greater. Hydrogen levels close to and below detection of 1ppm pose a problem and geothermometry should not be applied.

Comparing the HF1 data, the standard deviation for gas geothermometry is 47 ºC in contrast to 20 ºC for fluid inclusion Th values, indicating less precision for gas geothermometry than microthermometry. The average geothermometry temperature is 245 ºC in comparison to 182 ºC for the microthermometry; this temperature difference is excessive and is attributed to H_2 levels in HF1 that are close to or below the detection limit. Unlike the very low salinity geothermal systems on which geothermometry equations were based, HF1 has an approximate salinity of 8 eq. wt. % NaCl; this might explain the difference of the microthermometry and geothermometry data.

The Snowbird pegmatite quartz gas geothermometry values have a similar 1σ error for geothermometry based on both reactions, however, reaction 2 is closer to the Tt and is higher by 17 ºC. Gas geothermometry based on three gaseous species and elevated H_2 concentrations that could explain the improved accuracy of reaction 2. In addition, levels of H_2 well above the detection limit could explain a 23 to 25 ºC 1σ error that is about half that of Hansonburg fluorite. We also note that Snowbird fluid inclusions are hypersaline which might explain the difference between microthermometry and gas geothermometry.

CONCLUSIONS

1. The Ar/He vs. N_2/Ar plot does not have reactive species and therefore, unlike the CO_2/CH_4 vs. N_2/Ar plot of Norman (1997), offers a more reliable solution to the recognition of magmatic fluid sources.
2. Only magmatic fluids originating on convergent plate boundaries apply; fluids derived from basalts do not fit the diagram.
3. Data from meteoric sources can easily be differentiated from magmatic sources.
4. Fluid inclusion gas analyses can be used for geothermometry provided that: 1) no boiling occurred, 2) H_2 analyses are accurate, 3) fluid inclusions analyzed host the original trapped fluid chemistry and, 4) no organic material is present.
5. The gas geothermometry results for HF1 has more than twice the 1σ error of temperatures measured by microthermometry and is therefore less precise. Precision is improved for the Snowbird sample owing to good H_2 analysis.
6. The presence of salt decreases the accuracy of the gas geothermometer and a correction needs to be applied that incorporates fugacity of the species at equilibrium.

REFERENCES

Berndt, M.E., Allen, D.E., and Seyfried, W.E., 1996, Reduction of CO2 during serpentinization of olivine at 300 degrees C and 500 bar: Geology, v. 24, p. 351-354.

Blamey, N.J.F., 2000, The evolution of hydrothermal fluids at the Pipeline Gold Mine, Lander County, Nevada: unpublished Ph.D. Dissertation, New Mexico Tech, pp. 187.

D'Amore, F., and Panichi, C., 1980, Evaluation of deep temperatures of hydrothermal systems by a new gas geothermometer: Geochemica et Cosmochimica Acta, v. 44, p. 549-556.

Giggenbach, W.F., 1980, Geothermal gas equilibria: Geochemica et Cosmochimica Acta, v. 44, p. 2021-2032.

Giggenbach, W. F. , 1996, Chemical composition of volcanic gases: Monitoring and mitigation of volcano hazards, p. 221-256.

Henley, R.W., Truesdell, A.H., and Barton, P.B., 1984, Metals in hydrothermal fluids, *in* Fluid-mineral equilibria in hydrothermal systems: Society of Economic Geology Reviews in Economic Geology, v. 1, p. 115-127.

Nehring, N. L., and D'Amore, F., 1984, Gas chemistry and thermometry of the Cerro Prieto, Mexico, geothermal field: Geothermics, v. 13, no. 1-2, p. 75-89.

Norman, D.I., and Sawkins, F.J., 1987, Analysis of gases in fluid inclusions by mass spectrometer: Chemical Geology, v. 61, p. 110-121.

Norman, D.I., and Moore, J.N., 1997, Gaseous species in fluid inclusions: a fluid tracer and indicator of fluid processes [abs.]:European current research on fluid inclusions, No. XIV, Nancy, France, Abstracts, p. 243-244.

Norman, D.I., and Moore, J.N, 1999. Methane and Excess N_2 and Ar in geothermal fluid inclusions. Proceedings: Twenty-fourth Workshop of Geothermal Reservoir Engineering, Stanford University, Stanford, California, January 22-24, p. 233-240.

Prini, R.F., and Crovetto, R., 1989, Evaluation of data on solubility of simple apolar gases in light and heavy water at high temperature, J. Phys. Chem. Ref. Data, v. 18, p. 1231-1243.

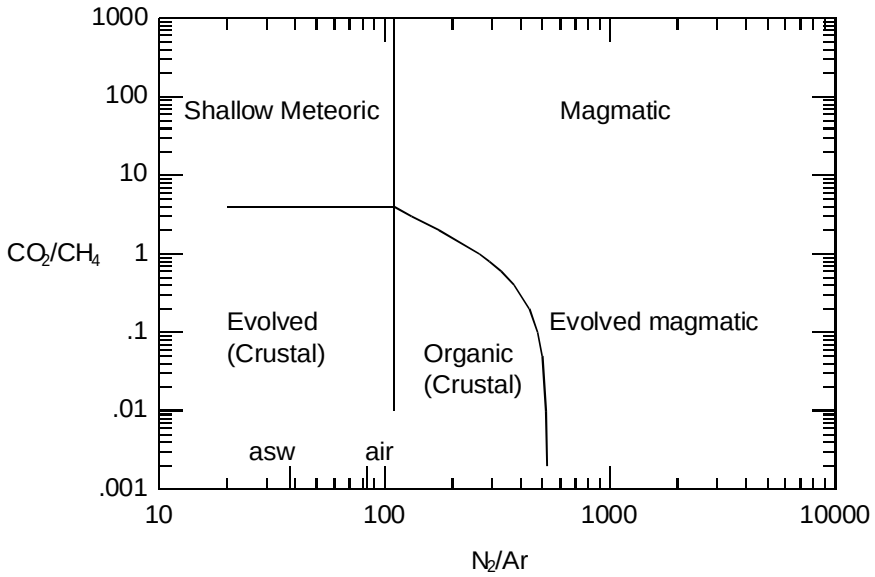

Figure 1. CO_2/CH_4 vs. N_2/Ar plot of Norman and Moore (1999).

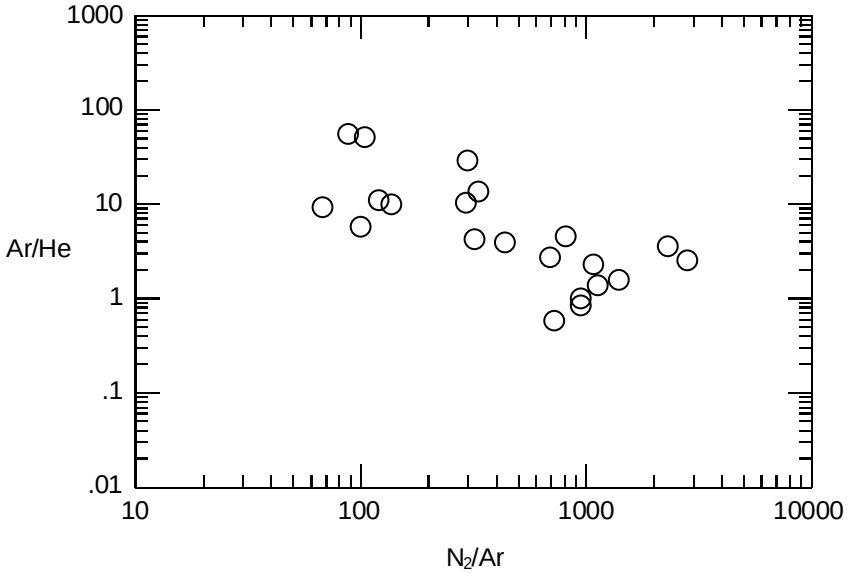

Figure 2. Compilation of Ar/He vs. N_2/Ar data for active volcanoes from Giggenbach (1996).

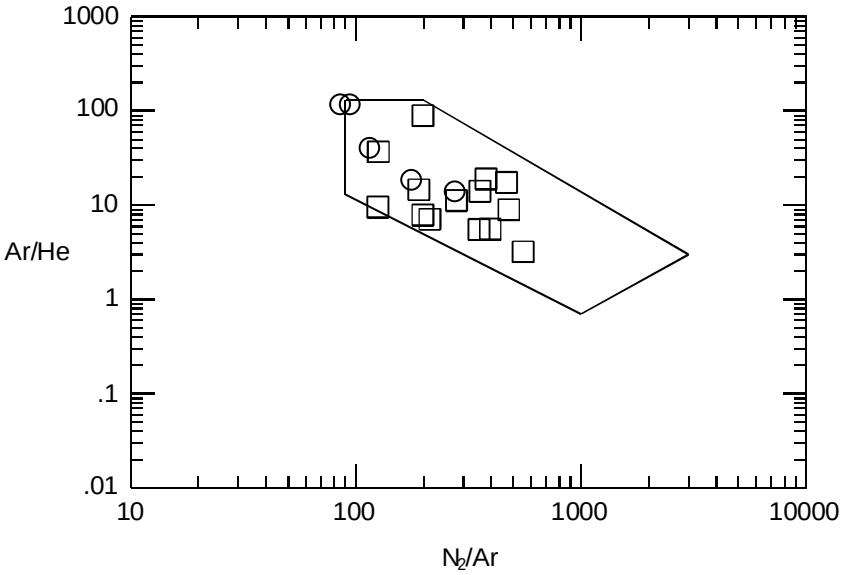

Figure 3. Ar/He plot of samples analyzed with our quadrupole mass spectrometer. Mt. Erebus anorthoclase in plotted in circles whereas Lowenstern's samples are in squares. A frame that defines Giggenbach's data is superimposed.

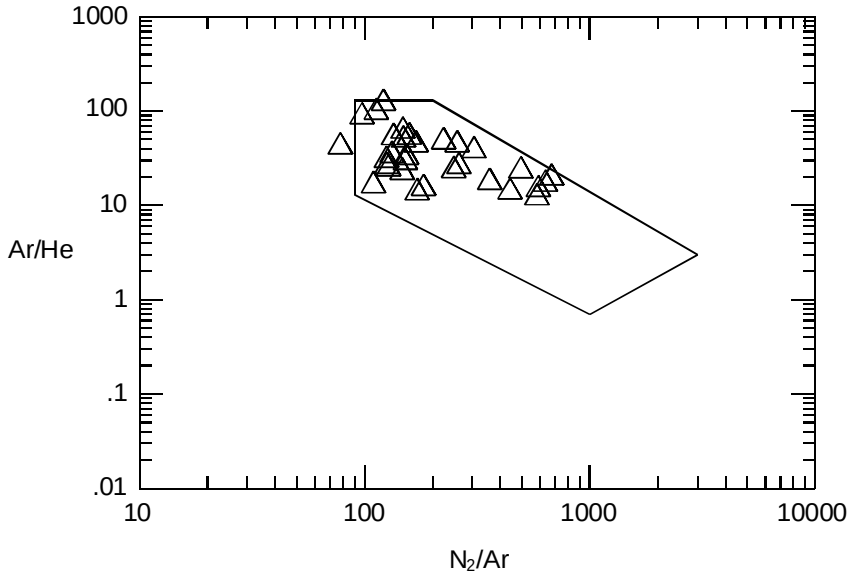

Figure 4. Ar/He vs. N_2/Ar plot for Coso samples collected at depths of 5300 to 10000 ft.

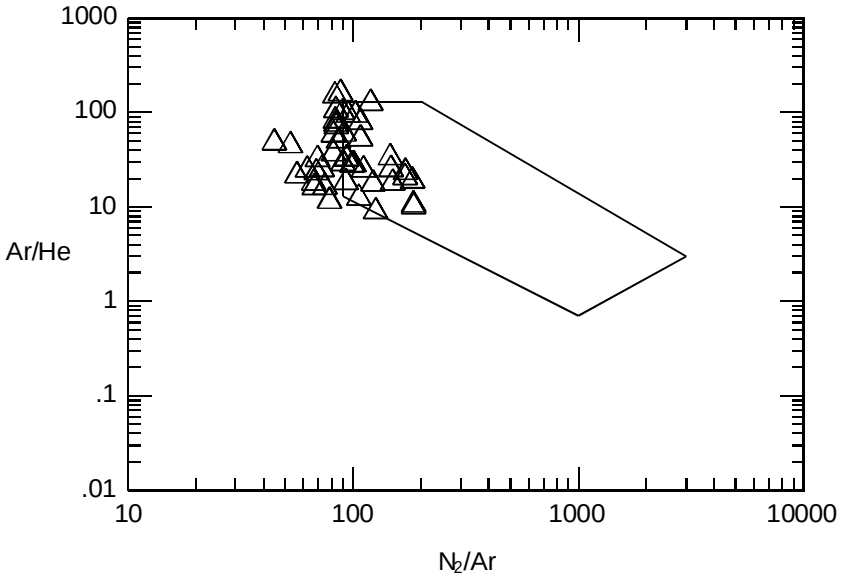

Figure 5. Ar/He vs. N_2/Ar plot for Karaha K-33. Data plots both within and outside the frame.

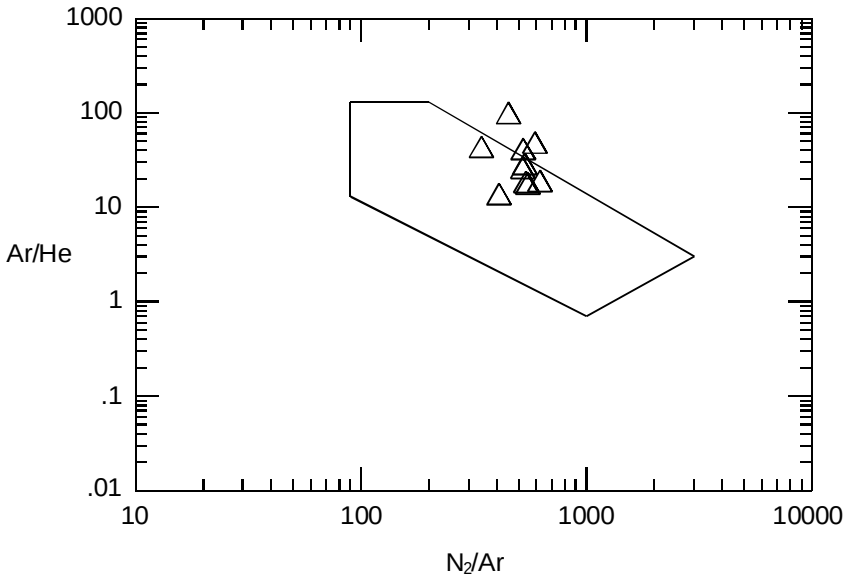

Figure 6. Ar/He vs. N_2/Ar plot for Darajat S3-6069E. Data plots both inside and above the frame.

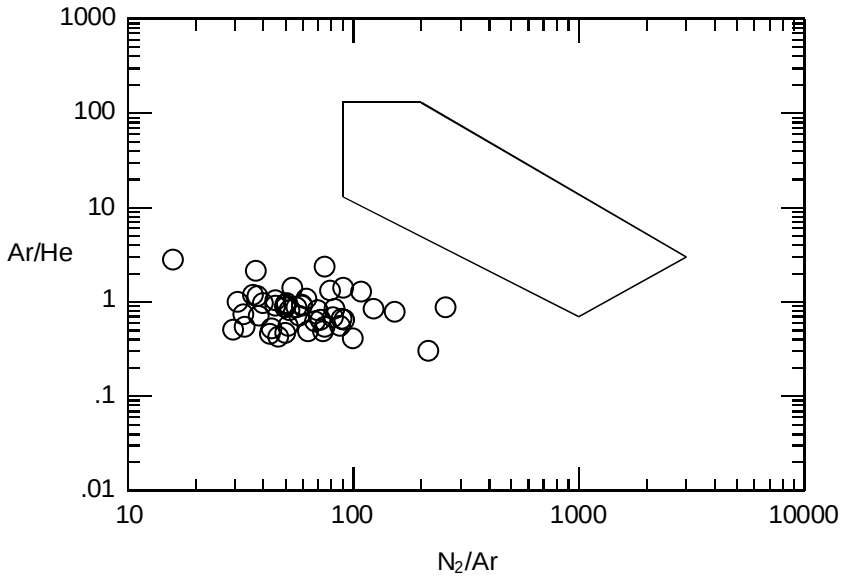

Figure 7. Ar/He vs. N_2/Ar plot for Hansonburg MVT fluorite. Data does not plot within the frame.